Fall 2010

Studies of Mono-Crystalline CVD Diamond Pixel Detectors

Stefan M Spanier
University of Tennessee - Knoxville, sspanier@utk.edu

Matt Hollingsworth
University of Tennessee - Knoxville, hollings@cern.ch

Studies of Mono-Crystalline CVD Diamond Pixel Detectors

W. Bugg, M. Hollingsworth, S. Spanier, Z. Yang

University of Tennessee, Knoxville, USA

E. Bartz, J. Doroshenko, D. Hits, S. Schnetzer, R. Stone, O. Atramentov, R. Patel, A. Barker

Rutgers University, Piscataway, USA

R. Hall-Wilton, V. Ryjov, C. Farrow

CERN, Geneva, Switzerland

M. Pernicka, H. Steininger

HEPHY, Vienna, Austria

W. Johns

Vanderbilt University, Nashville, USA

V. Halyo, B. Harrop, A. Hunt, D. Marlow, P. Hebda

Princeton University, Princeton, USA

Abstract

The Pixel Luminosity Telescope (PLT) is a dedicated luminosity monitor, presently under construction, for the Compact Muon Solenoid (CMS) experiment at the Large Hadron Collider (LHC). It measures the particle flux in several three layered pixel diamond detectors that are aligned precisely with respect to each other and the beam direction. At a lower rate it also performs particle track position measurements. The PLT's mono-crystalline CVD diamonds are bump-bonded to the same readout chip used in the silicon pixel system in CMS. Mono-crystalline diamond detectors have many attributes that make them desirable for use in charged particle tracking in radiation hostile environments such as the LHC. In order to further characterize the applicability of diamond technology to charged particle tracking we performed several tests with particle beams that included a measurement of the intrinsic spatial resolution with a high resolution beam telescope.

Keywords: diamond, spatial resolution, cms, pixel, luminosity, lhc

1. Introduction

The LHC will expose CMS to radiation levels as high as 2×10^{15} protons/cm^2 at the location of the innermost silicon pixel layer, r = 4 cm. The silicon detectors of CMS are designed to withstand the radiation at the highest luminosity for a time of three years. Under adverse beam conditions, with higher radiation levels their lifetime is reduced or they are damaged. It is therefore important to measure the radiation levels continuously in order to provide instrument protection via interlocks, to issue fast beam aborts (within 1 turn), and to monitor data for shifters to establish safe beam conditions. To achieve these goals, the Beam Radiation Monitoring (BRM) group of CMS has installed multiple instruments along the beam pipe that measure the particle flux inside the CMS detector, several of them based on mono- and poly-crystalline diamond detectors [1]. The next detector to be added into the BRM system is the Pixel Luminosity Telescope (PLT), which will specialize in luminosity measurements in addition to beam background measurements.

2. Pixel Luminosity Telescope

The PLT is a dedicated luminosity monitor for CMS based on mono-crystalline diamond pixel sensors. It consists of two arrays of eight small-angle telescopes situated one on each end of CMS. The PLT is designed to provide a high-precision measurement of the bunch-by-bunch relative luminosity at the CMS collision point on a time scale of a few seconds and a stable high-precision measurement of the integrated relative luminosity over the entire lifetime of the CMS experiment. Figure 1 shows a three dimensional design drawing of a PLT array. The telescopes consist of three equally-spaced planes of diamond

URL: mhollin3@utk.edu (M. Hollingsworth)

pixel sensors with a total telescope length of 7.5 cm. They are located 5 cm radially from the beam line at a distance of 1.8 m from the central collision point with a small angle pointing towards the collision point. The acceptance of the telescope can be changed towards particles travelling parallel to the beam by masking pixels.

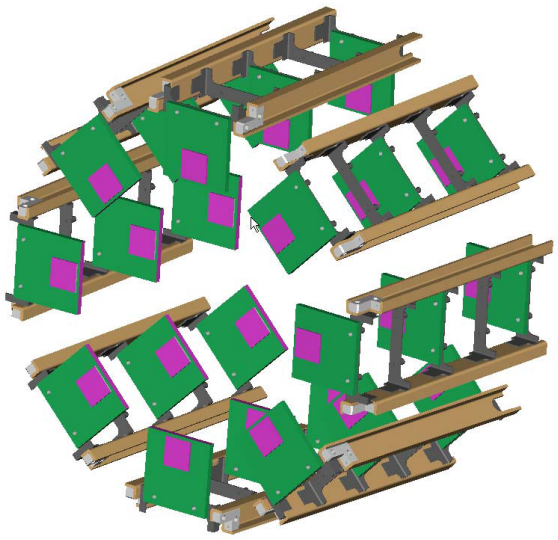

Figure 1: 3D design drawing of the telescope array at one side of the CMS detector, with the beam pipe in its center not shown. The length along the beam pipe between the outer two planes is 7.5 cm.

3. Mono-Crystalline Diamond Detector

Diamond sensors are crucial for the PLT application since they will operate efficiently with only moderate decrease in signal size over the entire lifetime of CMS [3]; they are capable of surviving up to 2×10^{15} protons/cm^2. Of equal importance, this radiation hardness does not require that the sensors be cooled. Furthermore, full charge collection occurs at an electric field of < 0.2 V/nm in approximately 1 ns/μm. Mono-crystalline diamond is used for the sensor material rather than poly-crystalline diamond since the pulse height distribution of mono-crystalline diamonds is shifted to higher values with the most-probable value more than twice as high and a decreased width, therefore well separated from zero, ensuring that any efficiency changes due to threshold drifts will be small [3].

4. Diamond Pixel Detector Readout

The telescope planes consist of mono-crystalline diamond sensors that are bump bonded to the PSI46.v2 CMS pixel readout chip [2].

The deposition of the pixel electrode pattern on the diamonds and the bump-bonding of the diamond sensors to the pixel readout chips were performed at the Princeton Institute of Science and Technology Materials (PRISM) micro-fabrication laboratory. Following surface preparation, electrodes were sputtered onto the diamond surface using a Ti/W alloy target as an under bump metalization (UBM). A 4 mm $\times$ 4 mm electrode was deposited on one side of the diamond using a shadow mask. On the other side, a pixel pattern was deposited using a standard lift-off photo-lithographic process. The pattern covered an area of 3.9 mm $\times$ 4.0mm and consisted of an array of 26 $\times$ 40 pixels with pitch of 150 μm $\times$ 100 μm matching that of the PSI46 chip.

The PSI46 chip features individual pixel threshold/mask settings, full analog readout of the pixel hit address and charge deposit, as well as a column-multiplicity signal (known as the Fast-OR), which indicates the number of double columns that had pixels over threshold in each bunch crossing. The primary luminosity measurement of the PLT is based on counting the number of telescopes with three-fold coincidences formed from the Fast-OR output. Fast-OR signals are read at the full bunch-crossing rate of 40 MHz clock, while the full pixel information, consisting of the row and column addresses and the pulse heights of all pixels over threshold, is read out at a lower rate of a few kHz. This full pixel readout provides tracking information and is a powerful tool for determining systematic corrections, calibrating pixel efficiencies and measuring the real-time location of the collision point centroid. The detector readout will be done in the same manner as the CMS pixel detectors are read out, which includes a Front End Driver (FED) and Front End Controller (FEC) [4].

5. PLT Performance Tests

In order to determine the performance of the diamond pixel sensors and the soundness of the PLT design, we carried out tests of a prototype telescope in the 150 GeV/c π^+ beam of the CERN SPS H4 beamline in May of 2009[6], and in 2010 in the 80 GeV/c proton beam in Fermilab's MTEST facility and with the 10 GeV/c proton/pion beam of the CERN PS. The primary goals were to determine: the yield of good pixel channels that result from the bump-bonding process, the pulse height response of the diamond sensors for minimum ionizing particles, the Fast-OR signal efficiency, and the tracking capability of the diamond pixel planes. Figure 2 shows a three-layer telescope used for the SPS and MTEST test beams. Small scintillators with an active area of 8 mm $\times$ 8 mm were positioned just upstream and downstream of the telescope. All of the results regarding the Fast-OR signals are based on events triggered by a coincidence of these two scintillators.

Before taking data, a procedure, similar to that for the CMS pixel detectors, was used to lower the pixel thresholds as much as possible. It utilizes the charge injection feature of the PSI46 pixel chip[2]: internally the readout chip could be programmed to deposit known amounts of charge into selected pixel channels. Iteratively we adjusted three parameters in the readout chip: the estimated average threshold, the trimming range around this setting, and the trimmed threshold for each individual pixel. The pixel thresholds achieved were in the range

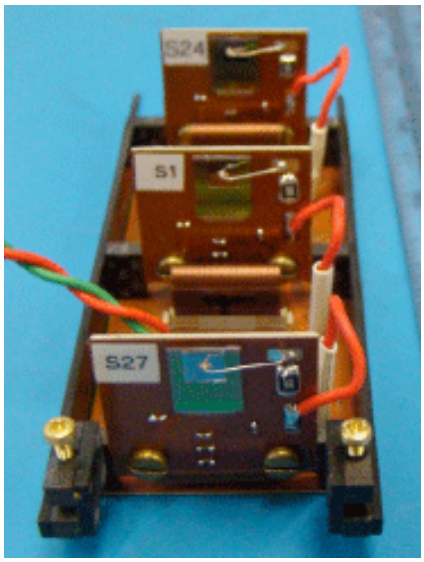

Figure 2: A fully assembled telescope. The diamond detector sits on top of the ROC and is attached to the high voltage supply wire.

between 2,500 and 4,500 electrons. The distribution of the turn-on points for each pixel before and after trimming is shown in Fig. 3.

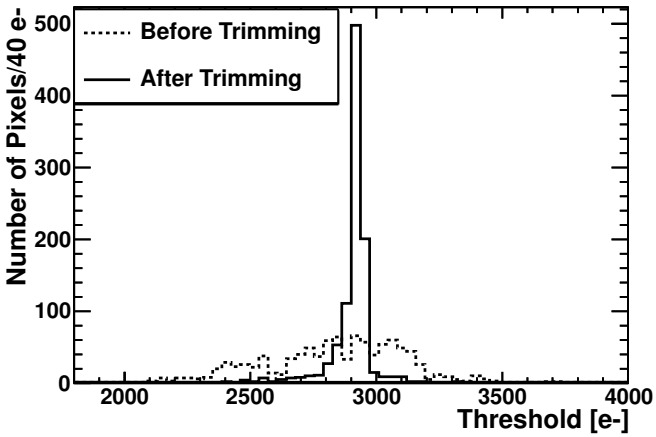

Figure 3: Distribution of turn-on points in units of collected electrons before and after trimming process.

The telescopes planes were also calibrated using the charge-injection capability of the PSI46 readout chip. For each pixel, the injected charge was ramped through the full input range while reading the corresponding output signal into the FED. The injected charge was plotted versus the FED ADC value and fit to a second-order polynomial to obtain a mapping from ADC count to pulse height in units of electrons. There is a 10% systematic uncertainty in charge calibration from plane to plane.

For determining charge deposit distributions, we defined an acceptance region which excluded rows or columns with noisy pixels. Figure 4 shows the measured charge distribution in units of collected electrons for single-hit charge clusters. The pulse height plotted is the sum over all neighboring pixels within the hit cluster. The most probable value was found to be 16,500 electrons. For comparison, the most probable signal for a 300 μm thick silicon sensor is 22,000 electrons.

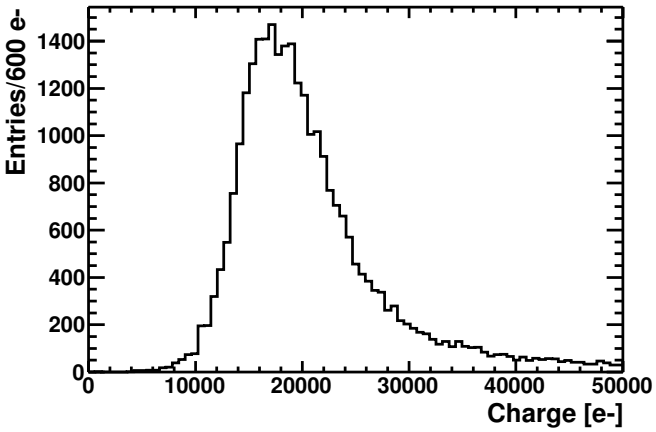

Figure 4: Summed charge distribution for the plane under test at the CERN PS, 10 GeV/c protons, for single-hit charge clusters. The MPV in units of collected electrons is 16,500.

6. Fast-OR Signal

The Fast-OR signals form the basis for the primary luminosity measurement of the PLT. Therefore, the measuring the timing response and efficiency is key to establishing their applicability for the PLT. While the Fast-OR output of the PSI46 chip was implemented for possible application in the Level 1 trigger, we present here the first systematic studies of this feature.

Timing and efficiency studies of the Fast-OR signals were performed at a beam test at Fermilab's MTEST using a beam with 80 GeV/c protons and at the CERN SPS with 120 GeV/c π+.

6.1. Timing

The timing was studied using a multi-hit TDC which measured the difference between the start of the ADC range in the FED that recorded the Fast-OR in 25 ns bins and the particle arrival, which was defined by the coincidence of two scintillators. The scintillator coincidence was used to trigger the readout of the FED. Both, the FED and the PLT utilize the same global system clock. Hence, this TDC configuration measured the phase between the arrival of a particle and the edge of the global clock. Due to the fixed phase between the trigger and the FED readout, all in-time Fast-OR signals should occur in the same time bin in the FED frame. Figure 5 shows the arrival times of the Fast-OR signals, as measured by the FED. As can be seen most events are in-time events in time-bin 3.

Due to time-walk, particles which arrive near the clock edge generate a Fast-OR signal either late or early. Late Fast-ORs

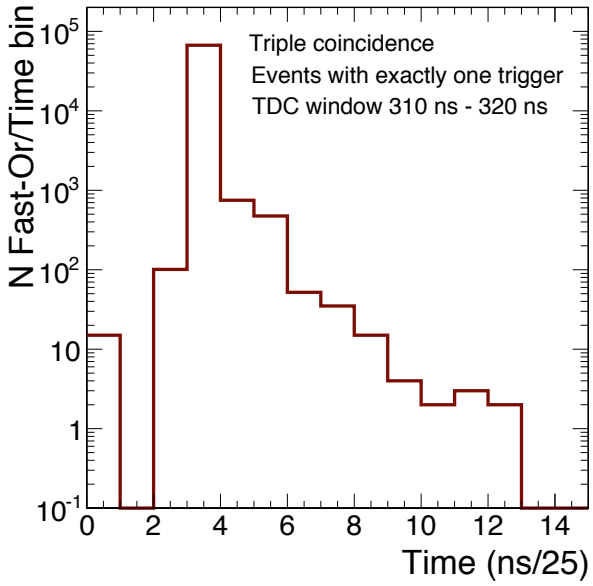

Figure 5: Arrival time of Fast-OR signal in the FED for all events within a TDC time window of 10ns about 5ns before the next clock cycle. In-time events occur in time-bin 3. Everything to the left of this bin is termed "early" and everything to the right is termed "late".

appear in a 25 ns time bin after the particle arrival in the scintillators, and early Fast-ORs appear in the time bin before the particle arrival. We found two cases: one with single late or early Fast-OR arrivals, called exclusive, and one with an in-time arrival together with a single arrival in a neighboring bin, called inclusive. The percentage occurrence of the late and early Fast-OR signals are summarized in Table 1. The exclusive Fast-OR events only affect the bunch-by-bunch luminosity measurement. The inclusive events additionally affect the integrated luminosity measurement. The time walk is related to the pulse-height of the signal which triggered the Fast-OR and the uncertainty of the particle arrival: a particle that arrived shortly after the leading clock edge and that had a large pulse height might be output one clock period earlier than the clock time of the trigger. Similarly, a particle that arrived shortly before the trailing clock edge and that had a small pulse height might be output one clock period later than the clock time of the trigger. The occurrences of such events will be suppressed in the LHC environment due to the particles arriving with a fixed phase with respect to the system clock.

	Exclusive	Inclusive
Early	0.13%	0.01%
Late	0.84%	0.38%

Table 1: Summary of the percentage of occurrence of early and late Fast-OR signals. The values for the late arrivals are upper limits due to contributions from late beam particles.

The early and late events were studied further by correlating the TDC information with the arrival time of the Fast-OR signal. The Fast-OR signals tagged as early indeed arrive near the edge of the clock. Late Fast-ORs arrive uniformly distributed in time. This is due to the equal probability of a low pulse height event occurring at any point in time in the 25 ns time bin.

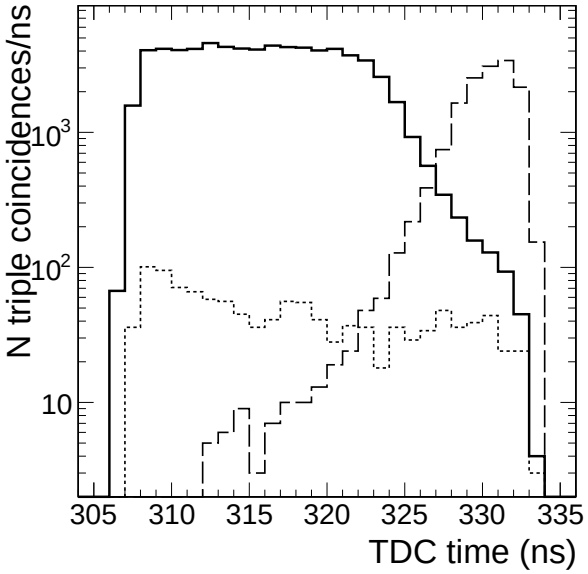

Figure 6: Fast-OR arrival time with respect to the clock edge, as measured by the TDC. The Fast-OR signals have been divided into in-time (solid line), early inclusive and exclusive (long dashed line), and late inclusive and exclusive (short dashed line) signals.

6.2. *Efficiency*

For determining the Fast-OR efficiencies we ensured that a particle passed through the enabled area of the plane under test: single clusters were required in each of the three planes and, for the two planes other than the one under study, the cluster positions were required to be in the central region excluding pixels rows and columns along the boundaries. Rows or columns with noisy pixels were found along the boundary and were excluded as well; this concerned at the most three rows or columns.

In order to correctly determine the Fast-OR efficiency using the test beam data, it is necessary to count Fast-OR signals that occur one clock period early or one clock period late as well as those that occur in-time. The correction due to accidental firing of the Fast-OR signal was found to be negligible. In the nine clock pulses occurring between 2.50 μs and 2.75 μs after a triggered event, there were 87 Fast-ORs out of 100,000 events giving a 0.03% probability for an accidental Fast-OR in a three clock period. The measured efficiencies for each plane were 99.3% for Plane 1, 99.6% for Plane 2, and 99.9% for Plane 3.

7. PLT Tracking and Alignment

In order to reconstruct tracks in the diamond pixel telescope, we first found the clusters associated with particle hits in each

plane. Pixels above threshold that were nearest neighbors in either the row or column direction were merged into clusters. For all studies regarding tracks we selected events that had only single clusters in each of the three planes. Events of this type constitute 89% of all events. About 70% of the events had one hit per cluster, 25% had two hits per cluster, and 5% had more than two hits per cluster. We excluded clusters with three or more pixels aligned in either a row or column. The cluster position was calculated as the average of the positions of its constituent pixels weighted by their collected charge.

We define the track residual as $\Delta x = x_2 - (x_3 - x_1)/2$, where x_1, x_2, and x_3 are the cluster hit positions in plane 1, 2, and 3, respectively. The relative offset of Plane 2 with respect to Planes 1 and 3 in terms of this residual is shown in Fig. 7. We find $\Delta x = 25\ \mu$m $\pm 5\ \mu$m in the column direction and $\Delta y = 146\ \mu$m $\pm 3\ \mu$m in the row direction. This is somewhat indicative of the the accuracy of the positioning of detectors onto the telescope planes and of the planes into the telescope during the assembly process. It is well within the requirements for the PLT. The figure also demonstrates that the alignment can be achieved to such a precision with few tracks.

8. Spatial Resolution

The spatial resolution was measured by utilizing a silicon micro-strip telescope provided by the University of Zürich [5] in the 10 GeV/c proton beam at the CERN PS. A single diamond pixel detector was placed in the center of the telescope between two entrance and two exit position modules, each providing an x and y coordinate. This silicon strip telescope has an intrinsic resolution of 2 μm per plane. However, due to multiple scattering effects the position uncertainty at the diamond detector of the reconstructed and selected particle tracks was about 4 μm. Residuals for the PLT were defined as $\Delta_x = x_{track} - x_{plt}$, where x_{track} is calculated from a linear fit to the hits in the silicon strip detectors, and x_{plt} is given as

$$x_{plt} = \frac{\sum_i^N (x_i \cdot Q_i)}{\sum_i^N Q_i} \quad (1)$$

with Q_i the charge in each pixel of the cluster in the PLT, col_i the column address of the pixel, and N the number of hits in the corresponding cluster. The y positions are calculated analogously. The x and y coordinates were treated independently. We apply a correction for non-uniform charge-sharing to the reconstructed hit position as function of the relative charge deposit in the neighboring pixels.

The x and y residuals for 2-hit clusters are shown in Fig. 8. We estimate the resolution from the RMS of theses distributions to be $\sigma_x = 29\ \mu$m (43 μm) and $\sigma_y = 23\ \mu$m (29 μm). The numbers in brackets are the expected corresponding resolutions for single hit clusters.

9. Conclusions

We have studied a prototype PLT telescope based on monocrystalline diamond pixel detectors in several test beams. The fraction of active pixel channels is high, 98% or more, in all three planes. The charge distribution has a most probable value of about 16,500 electrons, which is well above the average pixel threshold setting of 2,500 to 4,500 electrons. The efficiency of the Fast-OR signals that form the basis of the primary PLT luminosity measurement is greater than 99% for all three planes. Clear and well defined tracks are readily reconstructed in the telescope, which is a first for diamond pixel detectors. These results show that the PLT design concept is sound and that the project is ready to proceed. The PLT is on track for installation in CMS at the first shutdown, at which time it will become the largest utilization of diamond instrumentation in High Energy Physics.

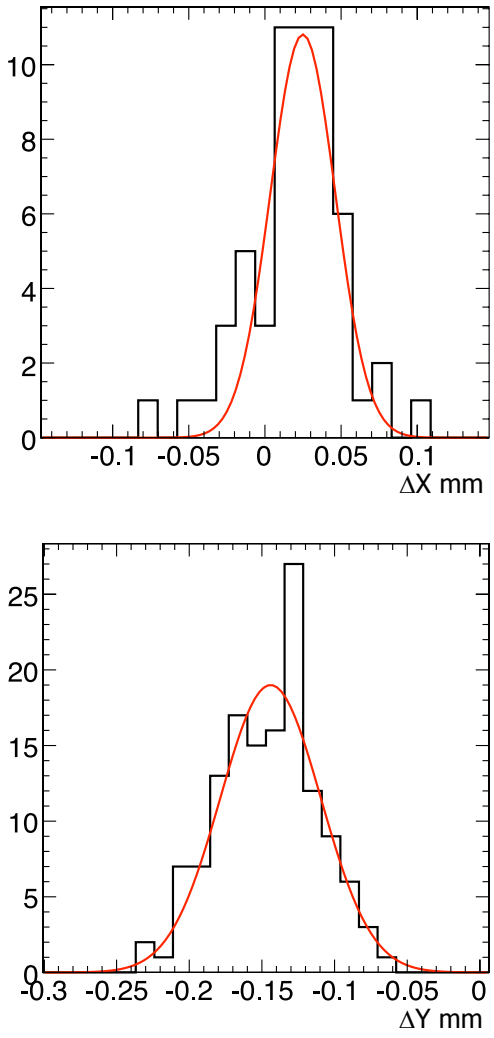

Figure 7: Residuals for tracks with > 2 hits per cluster, before alignment.

Acknowledgment

We thank the following people for their contributions to the PLT project: P. Butler, S.P.Lansley, and N. Rodrigues from Canterbury University; L. Lueking from Fermilab; S. Schmid

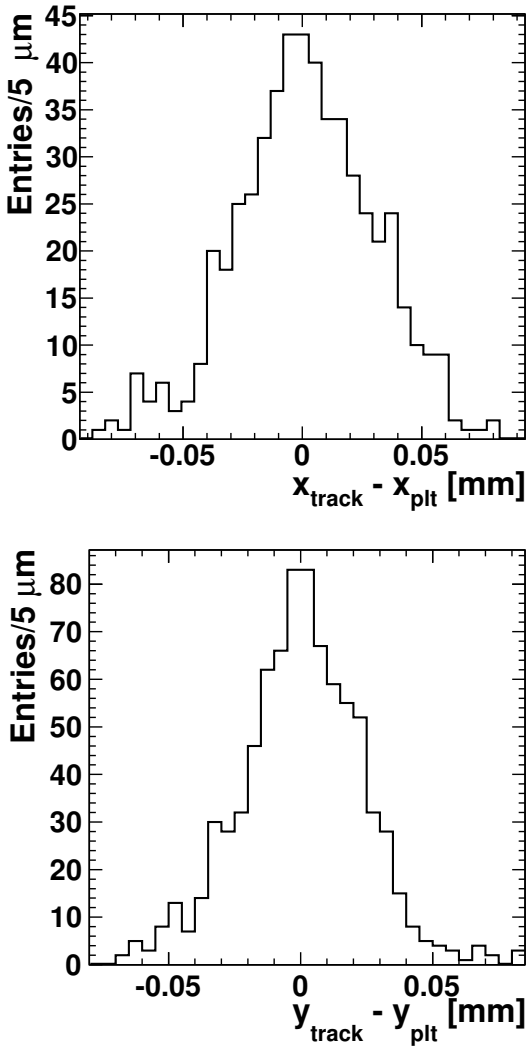

Figure 8: 2-hit residuals in x and y. For the x residuals, it was required that the hits in the cluster span two columns and no rows, whereas for the y residuals, the opposite was required.

from HEPHY Vienna; Y. Gershtein, E. Halkiadakis, and A. Lath from Rutgers University; B. Sands and D. Stickland from Princeton University; R. Lander from University of California, Davis; and B. Gabela from Vanderbilt University. We thank the staff of the Princeton Institute for the Science and Technology of Materials (PRISM) for their assistance with the bump bonding. We are grateful to the University of Zurich for lending us the strip detector telescope modules. Particularly, the support by C. Regenfus for the electronics readout and J. Rochet for machining a support for the telescope made this test beam possible. We are grateful to CMS Technical Coordination for assistance in launching and sustaining the project, particularly in its early phases. We thank the CERN PS accelerator test beam group and the Fermilab MTEST accelerator test beam group for their excellent operation.

References

[1] Bell, Alan. J., "'Beam & Radiation Monitoring for CMS,"' Nuclear Science Symposium Conference Record, 2008. NSS '08. IEEE , vol., no., pp.2322-2325, 19-25 Oct. 2008; W. Lohmann *et al.*, Fast Beam Conditions Monitor BCM1F for the CMS Experiment, Nucl. Instrum. Meth. A 614, 433 (2010).

[2] M. Barbero *et al.*, "'Design and test of the CMS pixel readout chip,"'Nucl. Instrum. Meth. A 517, 349 (2004).

[3] W. de Boer *et al.*, Radiation Hardness of Diamond and Silicon sensors compared. Phys. Stat. Sol. 204, 3004(2007).

[4] D. Kotlinski *et al.*, "'The control and readout systems of the CMS pixel barrel detector,"' Nucl. Instrum. Meth. A 565, 73 (2006).

[5] C. Amsler *et al.*, "A high resolution silicon beam telescope," Nucl. Instrum. Meth. A 480, 501-507 (2002).

[6] R.Hall-WIlton et al, "Results from a beam test of a prototype PLT diamond pixel telescope", Nucl. Instrum. Meth. A (2010) , doi:10.1016/j.nima.2010.04.097